

# Forecasting Liquidity Withdraw with Machine Learning Models

Haochuan (Kevin) Wang  
 Massachusetts Institute of Technology  
`hcw@mit.edu`

Aug 2025

## Abstract

Liquidity withdrawal is a critical indicator of market fragility. In this project, I test a framework for forecasting liquidity withdrawal at the individual-stock level, ranging from less liquid stocks to highly liquid large-cap tickers, and evaluate the relative performance of competing model classes in predicting short-horizon order book stress. We introduce the Liquidity Withdrawal Index (LWI)—defined as the ratio of order cancellations to the sum of standing depth and new additions at the best quotes—as a bounded, interpretable measure of transient liquidity removal.

Using Nasdaq market-by-order (MBO) data, we compare a spectrum of approaches: linear benchmarks (AR, HAR), and non-linear tree ensembles (XGBoost), across horizons ranging from 250 ms to 5 s. Beyond predictive accuracy, our results provide insights into order placement and cancellation dynamics, identify regimes where linear versus non-linear signals dominate, and highlight how early-warning indicators of liquidity withdrawal can inform both market surveillance and execution.

## 1 Introduction

Displayed liquidity in modern equity markets can vanish within seconds as market makers cancel quotes and widen spreads, especially around announcements or bursts of asymmetric order placement. Anticipating such withdrawal even a few seconds ahead is valuable for execution, market making, and risk management across participants. This paper develops a framework for *forecasting intraday liquidity withdrawal* at horizons from 250 ms to 5 s, using Nasdaq ITCH market-by-order (MBO) data and a set of econometric and machine learning models.

### 1.1 Liquidity Withdrawal Index (LWI)

We reconstruct the limit order book in real time, align order messages to a 250 ms grid, and define the Liquidity Withdrawal Index (LWI) as the fraction of liquidity removed at the top of book:

$$\text{LWI}_t = \frac{\text{Cancels}_t}{\text{MA}_{1s}(\text{DepthL1})_{t-1} + \max(\text{Adds}_t, \epsilon)}.$$

The denominator combines prior top-of-book depth with new additions, stabilized by a short moving average and a positive floor to avoid blow-ups in thin-book regimes. This interpretable, bounded index provides a real-time measure of order book fragility, directly tied to observable order flow.

### 1.2 Feature Construction

From the MBO stream we construct features including spreads at multiple depths, top-of-book depth, order flow imbalance (OFI), queue imbalance (QI), rolling means and volatilities, and activity rates (adds/-cancels per second). These features capture both the state and dynamics of the book. A cross-ticker feature screening procedure yields a *consensus* set dominated by short-horizon LWI lags and rolling volatilities of spread, depth, and order flow.

### 1.3 Model Classes

We compare two families of models across horizons of 250 ms, 1 s, 2 s, and 5 s: (i) linear baselines, AR(5) and HAR, which provide interpretable and latency-friendly forecasts; (ii) non-linear tree ensembles (XGBoost), which capture threshold effects and feature interactions. Evaluation uses walk-forward cross-validation with an embargo to mitigate information leakage and mimic real-time deployment.

### 1.4 Contributions and Positioning

We contribute a reproducible pipeline from raw MBO events to a stabilized LWI target and feature panel, and benchmark linear versus tree-based models under realistic evaluation. Results show horizon-dependent structure: 250 ms is noise-dominated; linear models perform best at 1–2 s; and tree ensembles dominate at 5 s. Unlike most LOB prediction studies that focus on mid-price direction, we target *liquidity withdrawal*, aligning the analysis with operational priorities in execution and surveillance. Figure 1 illustrates clustered LWI spikes for RKLB on July 30, 2025, around 14:10 ET, coinciding with abrupt price gaps. Anticipating such withdrawal would allow market makers to adjust spreads or inventories proactively, reducing adverse selection risk.

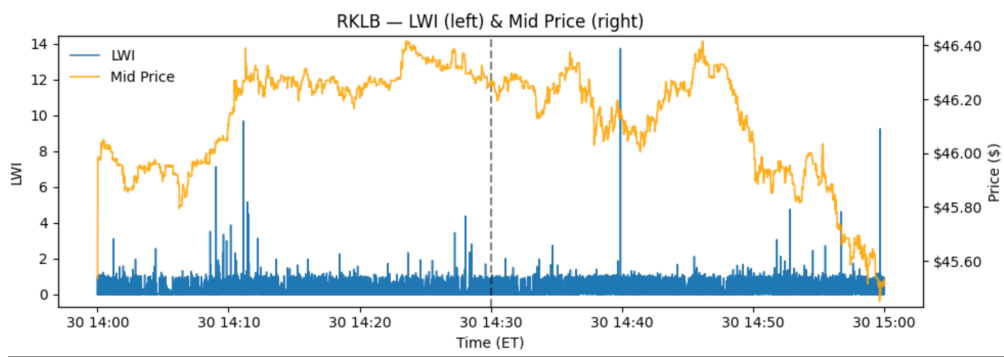


Figure 1: Liquidity withdrawal and stock prices of RKLB on July 30, 2025.

## 2 Literature Review

### 2.1 Liquidity, resiliency, and event-time dynamics

Market quality is often summarized by spread, depth, and resiliency [1, 2]. Spread (bid–ask tightness) and depth (available volume) are widely studied, while resiliency—the speed of liquidity recovery after shocks—captures how quickly the book replenishes [2]. Event studies consistently show that liquidity providers withdraw quotes just before and during announcements, then normalize afterward. For example, high-frequency traders widened bid–ask spreads before macroeconomic releases and reduced depth immediately after, with reversion occurring within minutes [3]. Our Liquidity Withdrawal Index (LWI) formalizes this transient withdrawal phase at sub-second resolution, providing an interpretable, bounded measure of book fragility that can be forecast and monitored in real time.

### 2.2 Working with MBO data in a low SNR regime

Market-by-order (MBO) feeds provide granular detail on order flow (adds, cancels, replacements) but are noisy: bursts, flickering quotes, and irregular event timing. Effective engineering requires: (i) *clocking* irregular events to a uniform grid without aliasing fast dynamics—often done by resampling to fixed bars [4]; (ii) *stabilizing* denominators to prevent ratio blow-ups in thin books; and (iii) *filtering* via rolling means and variances to boost signal-to-noise [5, 6]. In line with this literature, our pipeline uses a 250 ms grid with a warm start, denominator flooring, and rolling statistics to suppress flicker and heteroskedastic bursts before modeling.

## 2.3 Model selection

We evaluate two families of models, chosen to balance interpretability, predictive power, and latency.

**Linear baselines: AR and HAR.** Autoregressive (AR( $p$ )) models are simple and latency-friendly. We use AR(5), which provides a one-second lookback to capture short-term linear dependence in liquidity withdrawal. The Heterogeneous Autoregressive (HAR) model extends AR by including multi-scale aggregates (1 s/10 s/60 s) [7, 8]. HAR improves performance at intermediate horizons (e.g., 2 s), but at longer horizons (5 s) the model struggles as non-linear dependencies grow more important [9].

**Tree ensembles and threshold effects.** Gradient-boosted decision trees (XGBoost) capture conditional thresholds and feature interactions efficiently. Prior work shows boosted trees outperform linear models for order-book forecasting by exploiting non-linear dependencies [9]. In our results, XGBoost significantly outperforms AR/HAR at 5 s horizons, consistent with the growing role of non-linear structure in driving liquidity withdrawal.

## 2.4 Positioning and implications

Unlike much of the LOB prediction literature focused on mid-price direction [10], we target *liquidity withdrawal* directly, through a ratio observable from cancels and adds. This target is interpretable and operational: predictions map to a tangible phenomenon that market participants can act upon. Our comparisons suggest that AR/HAR are adequate at 1–2 s horizons, while boosted trees dominate at 5 s, and no model delivers robust predictability at 250 ms. These findings translate into actionable design principles for execution and surveillance systems, where early warning of transient liquidity stress is most valuable.

## 3 Data Set

We use Market-by-Order (MBO) data for U.S. equities from Databento.<sup>1</sup> MBO provides the full order flow — every add, cancel, replace, and trade message from the NASDAQ matching engine — at nanosecond resolution. For tractability, our study focuses on July 30, 2025, 14:00–15:00 ET, covering several actively traded symbols (e.g., HIMS, NBIS, RKLB, SNAP). After aligning messages to a 250 ms Eastern Time grid and reconstructing the top of book, and within 1 hour we obtain a panel of roughly 14,400 observations per symbol. This resampling captures sub-second dynamics while taming the burstiness of raw event time.

From the resampled book we construct both the target, the Liquidity Withdrawal Index (LWI), and a panel of microstructure features: spread and depth at level 1, order and queue imbalances (OFI, QI), rolling means and volatilities of mid-price returns, and add/cancel rates. These engineered features provide interpretable summaries of state, flow, and short-term volatility. A full list of raw MBO fields and the derived feature definitions is provided in Appendix 6.

## 4 Methods

Our methodology follows a pipeline from raw MBO data to engineered features, then to model estimation and evaluation across multiple horizons. The design emphasizes predictive accuracy while maintaining robustness and low latency in high-noise, high-frequency settings.

### 4.1 Data Preparation

We reconstruct the limit order book from Databento Market-by-Order (MBO) events and resample all messages onto a uniform 250 ms Eastern Time (ET) grid. This step aligns the inherently irregular event stream and avoids aliasing ultrafast bursts. It also facilitates modeling by producing equally spaced time-series suitable for both linear and non-linear estimators.

---

<sup>1</sup><https://databento.com/portal/catalog/us-equities>

From the reconstructed book, we compute a panel of features commonly used in market microstructure research: bid–ask spread, top-of-book depth, order flow imbalance (OFI), queue imbalance (QI), rolling means and standard deviations of LWI and QI, realized variance proxies, and activity rates (adds/cancels). Feature selection combines mutual information, gradient-boosted tree importance, and LASSO, yielding a consensus set dominated by short-horizon LWI lags, moving averages, and volatility measures.

## 4.2 Feature Selection Framework

Because high-frequency order flow is noisy and collinear, feature selection must balance stability with interpretability. We therefore evaluate each feature’s informativeness using three complementary methods:

**Mutual Information (MI).** MI measures general dependence between feature  $X$  and target  $Y$ , capturing both linear and non-linear associations. For LWI, MI identifies which features carry the strongest predictive content regardless of functional form.

**XGBoost Feature Importance.** Tree ensembles rank features by their marginal contribution to predictive accuracy. XGBoost is particularly well suited to detect threshold effects such as “if queue imbalance is extreme and depth collapses, withdrawal rises.”

**LASSO Regression.** The  $\ell_1$  penalty of LASSO enforces sparsity, shrinking weak predictors to zero and highlighting features with stable linear contributions. A feature that consistently ranks highly across all three approaches is considered robust and included in the consensus panel.

## 4.3 Consensus Across Tickers

We apply the selection framework at the 1-second horizon across four active tickers and aggregate the results. Table 1 reports, for each feature, the number of symbols in which it appears among the top predictors, its mean rank, and total method hits. Consensus features are those appearing in at least 60% of tickers.

Feature	$n_{\text{symbols}}$	Mean	Best Rank	Method Hits	Consensus
LWI_ma1s	4	1.00	12	Yes	
LWI_lag1	4	1.00	8	Yes	
LWI_sd1s	4	2.00	10	Yes	
dLWI_1s	4	2.50	12	Yes	
LWI_lag2	4	2.75	8	Yes	
adds_rate1s	4	5.00	8	Yes	
canc_rate1s	4	5.75	6	Yes	
QI_lag1s	4	5.75	4	Yes	
depth_L1_lag1s	4	5.75	4	Yes	
depth_L1_lag4	4	6.00	4	Yes	
QI_sd1s	4	6.25	6	Yes	
LWI_ma10s	4	6.75	5	Yes	
QI_lag4	4	6.75	4	Yes	
LWI_ma2s	4	8.00	6	Yes	
LWI_sd2s	3	7.00	4	Yes	
spread_sd1s	3	8.00	5	Yes	

Table 1: Consensus feature selection across four symbols at the 1-second horizon.

## 4.4 Stationarity and Persistence

We test whether the Liquidity Withdrawal Index (LWI) is stationary using the Augmented Dickey–Fuller (ADF) test. Across all four tickers, the ADF statistics are strongly negative with p-values near zero (Table 2), rejecting the unit root null. Thus, LWI is stationary, making it valid for autoregressive modeling without

differencing. Autocorrelation plots reveal significant dependence at the first one or two lags, followed by rapid decay. This pattern is consistent with a stationary but short-memory process: shocks to liquidity withdrawal are temporary but persist briefly, reinforcing the use of short lags as predictive signals.

Symbol	ADF statistic	p-value
HIMS	-17.97	$2.79 \times 10^{-30}$
NBIS	-13.61	$1.88 \times 10^{-25}$
RKLB	-11.89	$6.03 \times 10^{-22}$
SNAP	-12.71	$1.01 \times 10^{-23}$

Table 2: ADF test results for LWI stationarity.

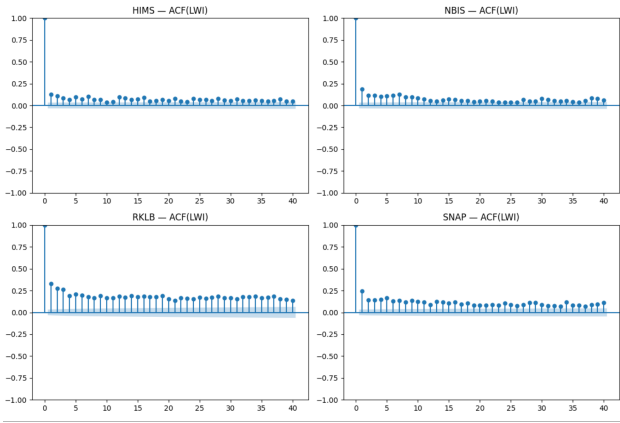


Figure 2: ACF and PACF of LWI across four tickers, showing short-memory dynamics.

## 4.5 Evaluation Protocol

We apply walk-forward cross-validation with an embargo period to prevent information leakage. Each split trains on earlier intervals and tests on later ones, emulating live deployment. Models are evaluated using  $R^2$  and RMSE across folds and horizons. Reporting horizon-specific performance reveals which models dominate at different timescales: linear AR/HAR at 1–2 s, XGBoost at 5 s, and minimal predictability at 250 ms where noise dominates.

## 4.6 Summary of Design Choices

Our pipeline integrates production constraints with research aims: (i) **Uniform resampling and filtering** stabilize noisy MBO streams. (ii) **Consensus features** ensure robustness across tickers. (iii) **Linear models** capture short-memory dependencies in LWI. (iv) **Boosted trees** provide a flexible non-linear benchmark. Together, these design choices allow us to characterize when linear vs. non-linear structure dominates and how feature-engineered predictors translate into operationally relevant liquidity withdrawal forecasts.

# 5 Results

## 5.1 Evaluation Protocol

We use a five-fold expanding-window walk-forward split with an embargo buffer to prevent look-ahead bias. In each fold, models are trained on all prior data and tested on the next out-of-sample block, mirroring live deployment.

Targets are defined as the mean Liquidity Withdrawal Index (LWI) over the next  $k$  bins, where  $k = 1$  for 250 ms and  $k = 20$  for 5 s. Thus, 250 ms corresponds to a one-step forecast, while 5 s is a many-step forecast. Benchmarks follow our implementation:

- AR(5): short-memory autoregression with lags up to 1 s.
- HAR: heterogeneous autoregression with aggregates at 250 ms, 2 s, and 10 s.
- XGB: boosted trees on lagged and rolling engineered features.

## 5.2 Performance Across Models and Horizons

Table 3 summarizes mean out-of-sample  $R^2$  by symbol, model, and horizon. Patterns are clearly horizon-dependent:

- At 250 ms, all models perform poorly due to noise.
- At 1–2 s, HAR improves on AR by incorporating multi-scale aggregates.
- At 5 s, XGB dominates with  $R^2$  above 0.90 for most tickers, capturing nonlinear interactions that linear models miss.

Symbol	Model	250 ms	1 s	2 s	5 s
AAPL	AR(5)	-0.146	0.468	0.632	-0.684
	HAR	-0.008	0.527	0.850	0.727
	XGB	<b>0.006</b>	<b>0.786</b>	<b>0.862</b>	<b>0.950</b>
NVDA	AR(5)	-0.294	0.462	0.649	-1.245
	HAR	<b>0.053</b>	0.640	0.904	0.799
	XGB	0.049	<b>0.843</b>	<b>0.913</b>	<b>0.963</b>
TSLA	AR(5)	-0.098	0.499	0.658	-0.270
	HAR	-0.043	0.519	<b>0.850</b>	0.735
	XGB	-0.225	<b>0.706</b>	0.822	<b>0.936</b>
HIMS	AR(5)	-0.023	0.533	0.681	0.061
	HAR	-0.006	0.466	<b>0.821</b>	0.653
	XGB	-0.053	<b>0.677</b>	0.777	<b>0.892</b>
NBIS	AR(5)	0.002	0.587	0.743	0.294
	HAR	<b>0.034</b>	0.546	<b>0.866</b>	0.731
	XGB	-0.209	<b>0.689</b>	0.838	<b>0.938</b>
RKLB	AR(5)	-0.060	0.544	0.715	-0.053
	HAR	<b>0.006</b>	0.539	<b>0.867</b>	0.723
	XGB	-0.057	<b>0.776</b>	0.859	<b>0.930</b>
SNAP	AR(5)	-0.022	0.545	0.699	0.147
	HAR	<b>0.012</b>	0.497	<b>0.837</b>	0.703
	XGB	-0.142	<b>0.761</b>	0.849	<b>0.931</b>

Table 3: Out-of-sample  $R^2$  across models (AR(5), HAR, XGB) and horizons (250 ms–5 s). Bold values indicate the best model per symbol-horizon.

## 5.3 Boosted Trees Diagnostics

Gradient-boosted trees deliver the strongest performance at multi-second horizons. At 1 s, XGB outperforms AR/HAR but underpredicts sharp cancellation spikes, producing right-skewed residuals. At 5 s, temporal aggregation smooths noise and residuals become symmetric and centered, indicating better calibration.

Two adjustments improve short-horizon accuracy: (i) spike-aware losses (Huber, quantile, or Box–Cox targets) to reduce underprediction of extreme withdrawals; (ii) stress-sensitive features (depth drawdowns, cancel/replace bursts) to capture imminent liquidity shocks.

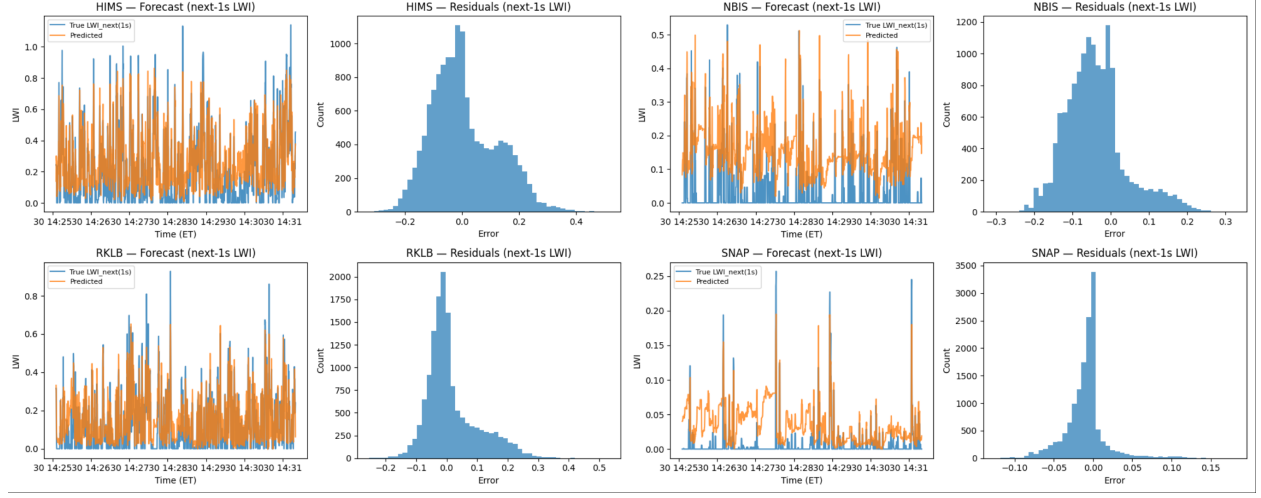


Figure 3: XGB one-second LWI forecast.

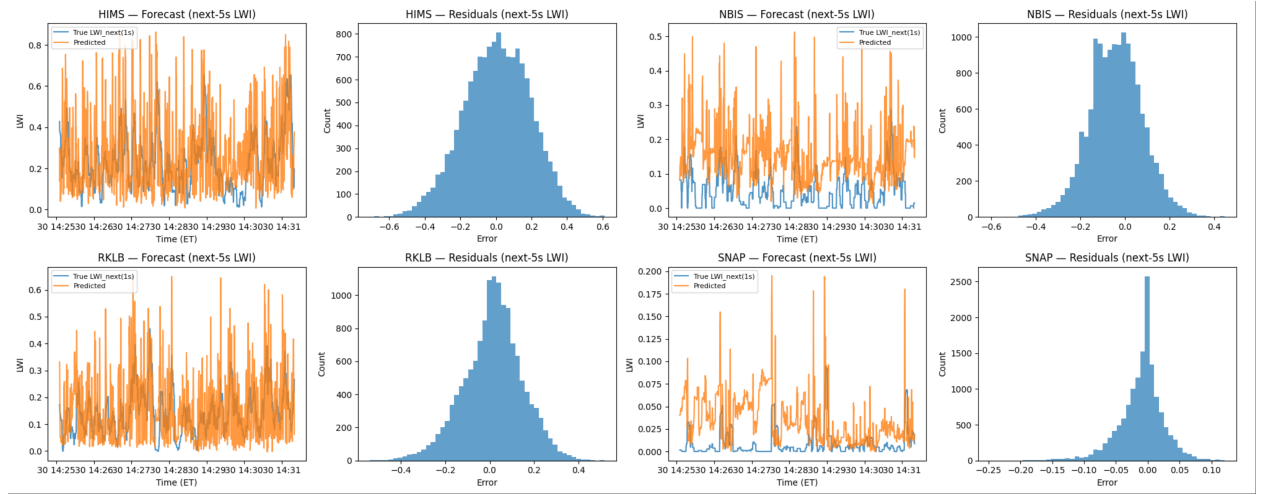


Figure 4: XGB five-second LWI forecast. Temporal aggregation yields higher  $R^2$  and near-symmetric residuals, indicating improved calibration.

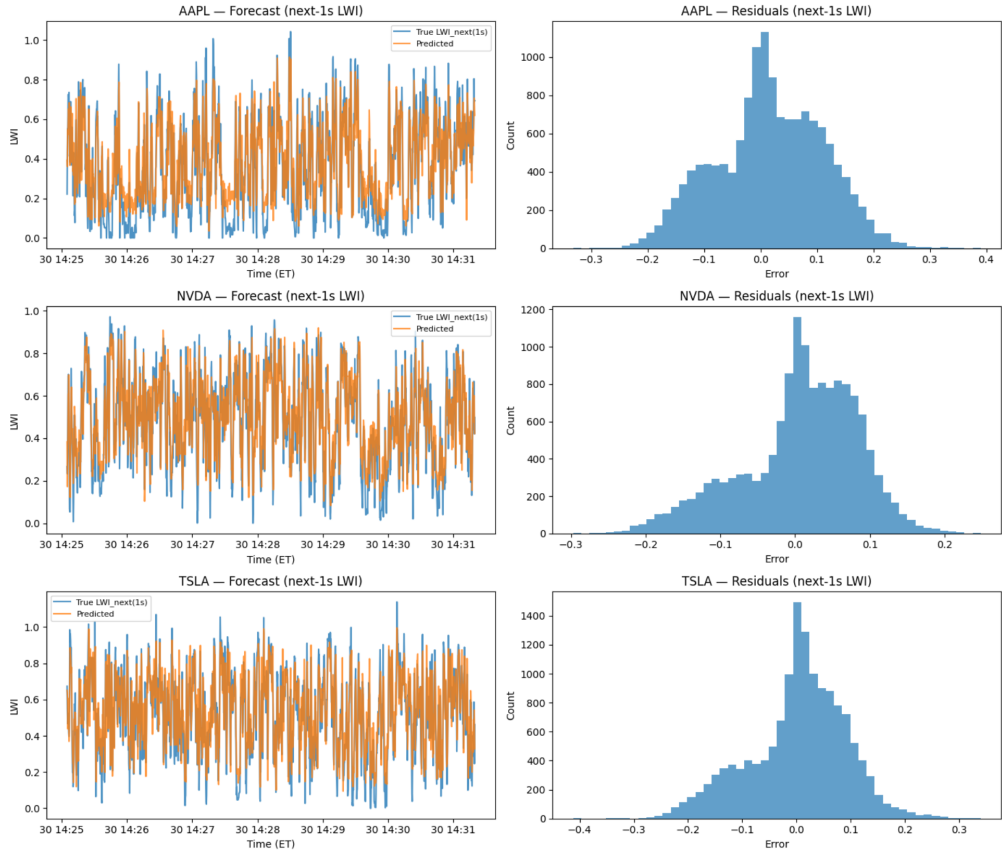


Figure 5: **XGB one-second LWI forecasts.** For highly liquid tickers such as AAPL, NVDA, and TSLA, residuals are less skewed even at the 1s horizon. This suggests fundamental differences in risk dynamics across liquidity tiers, motivating specialized models for distinct liquidity clusters rather than a uniform approach.

## 6 Conclusion

We propose and evaluate a framework for forecasting liquidity withdrawal using Nasdaq MBO data and a Liquidity Withdrawal Index (LWI). Results across seven tickers show a horizon-dependent structure: short-memory lags make AR and HAR competitive at 1–2s, while nonlinear dependencies dominate at 5s, where XGBoost achieves  $R^2$  above 0.90. These findings confirm that liquidity withdrawal combines linear persistence with nonlinear regime shifts, and that tree ensembles already provide strong practical benchmarks.

Given this performance, the usefulness of deep sequence models with many layers is unclear: their complexity, latency, and overfitting risk offer little advantage over boosted trees. Future research should instead explore lightweight, shallow networks or hybrid designs that retain interpretability and low latency while modestly extending predictive power. Such models could clarify whether sequential learning adds incremental value beyond strong tree-based baselines in forecasting liquidity withdrawal and related market fragility proxies.

## References

- [1] O’Hara, M. (1995). *Market Microstructure Theory*. Blackwell.
- [2] Foucault, T., Pagano, M., & Röell, A. (2013). *Market Liquidity: Theory, Evidence, and Policy*. Oxford University Press.
- [3] Hautsch, N., & Huang, R. (2012). *The Market Impact of Macroeconomic News Announcements*. European Central Bank Working Paper. <https://www.econstor.eu/handle/10419/154626>
- [4] Menkveld, A. J., & Yueshen, B. (2019). *The Flash Crash: A Cautionary Tale About Highly Fragmented Markets*. SSRN. <https://arxiv.org/abs/1904.05321>
- [5] Zhang, X., & Chan, N. (2020). *Noise Reduction in High-Frequency Limit Order Book Data*. arXiv preprint. <https://arxiv.org/abs/2001.09031>
- [6] Kercheval, A., & Zhang, Y. (2015). *Modeling High-Frequency Limit Order Book Dynamics with Machine Learning*. arXiv preprint. <https://arxiv.org/abs/1502.04574>
- [7] Corsi, F. (2009). *A Simple Approximate Long-Memory Model of Realized Volatility*. Journal of Financial Econometrics, 7(2), 174–196.
- [8] Corsi, F. (2004). *A Simple Long Memory Model of Realized Volatility*. SSRN. <https://ssrn.com/abstract=626364>
- [9] Yu, S., & Liu, Y. (2019). *Comparative Study of Machine Learning Methods for High-Frequency Limit Order Book Prediction*. arXiv preprint. <https://arxiv.org/abs/1905.10428>
- [10] Ntakaris, A., Kanniainen, J., Gabbouj, M., & Iosifidis, A. (2018). *Benchmark Dataset for Mid-Price Forecasting of Limit Order Book Data with Machine Learning Methods*. Journal of Data, Information and Management, 2(1), 1–12.

## Appendix A: Raw MBO Data Fields

The raw Market-by-Order (MBO) dataset from Databento contains the following fields:

Field	Description
ts_recv	Capture-server-received timestamp, in nanoseconds since UNIX epoch.
ts_event	Matching-engine-received timestamp, in nanoseconds since UNIX epoch.
ts_in_delta	Matching-engine-sending timestamp expressed as nanoseconds before ts_recv.
channel_id	Channel ID assigned by Databento (incrementing integer starting at zero).
publisher_id	Publisher ID assigned by Databento, denoting dataset and venue.
instrument_id	Numeric instrument identifier.
symbol	Symbol of the instrument.
sequence	Message sequence number assigned at the venue.
order_id	Unique order ID assigned at the venue.
price	Order price, stored as an integer where one unit equals $10^{-9}$ (i.e., \$0.000000001).
size	Order quantity.
side	Side of the event: Bid (buy), Ask (sell), or None if unspecified.
action	Event type: Add, Cancel, Modify, Clear Book, Trade, Fill, or None.
rtype	Record type (each schema corresponds to one value).
flags	Bit field indicating event end, message characteristics, and data quality.

Table 4: Raw Market-by-Order (MBO) data fields as provided by Databento.